

NUMERICAL SOLVER FOR VERTICAL AIR MOTION ESTIMATION

*Salcedo-Bosch, A.¹, Domínguez-Pla, P.¹, Rocadenbosch, F.^{1,2}, Senior Member, IEEE,
Frasier, S. J.³, Senior Member, IEEE*

¹CommSensLab-UPC, Department of Signal Theory and Communications (TSC), Universitat Politècnica de Catalunya (UPC)

²Institut d'Estudis Espacials de Catalunya (Institute of Space Studies of Catalonia, IEEC), Barcelona, Spain, E-08034 Barcelona, Spain

³Microwave Remote Sensing Laboratory, University of Massachusetts, Amherst, MA 01003-9284

ABSTRACT

We present preliminary research on a method to estimate Vertical Air Motion (VAM) at a particular height by comparing the measured rain-rate (RR) by a vertically-pointing S-band Frequency-Modulated Continuous-Wave (FMCW) radar with that of a ground-based disdrometer. The method is based on a constrained parametric solver, assuming high correlation between 5-min averaged rain rates measured by the radar and disdrometer. The method is tested over disdrometer and radar observations during the Verification of the ORigins Tornado EXperiment in South East US (VORTEX-SE) project. Finally, the results are partially validated by means of fitting a gamma distribution to the VAM-corrected DSD profiles and studying its parameters.

Index Terms— Vertical Air Motion, S-Band radar, Rain Rate, Drop Size Distribution

1. INTRODUCTION

Several different ground-based remote sensing instruments are able to assess temperature and/or humidity profiles in the boundary layer including infrared spectrometers and microwave radiometers [1]. However, these instruments have a common drawback, which is their poor performance under precipitation scenarios. Alternatively, lower microwave frequency radar observations are mostly unaffected during precipitation, and hence, they emerge as an alternative in order to reveal details regarding precipitation microphysical processes [2]. Among the distinct radar technologies available, the S-band (~ 10 cm) Frequency-Modulated Continuous Wave (FMCW) radar has been used to monitor boundary layer features since the 1960s [3].

This research is part of the projects PGC2018-094132-B-I00 and MDM-2016-0600 (“CommSensLab” Excellence Unit) funded by Ministerio de Ciencia e Investigación (MCIN)/ Agencia Estatal de Investigación (AEI)/ 10.13039/501100011033/ FEDER “Una manera de hacer Europa”. The work of A. Salcedo-Bosch was supported under grant 2020 FISDU 00455 funded by Generalitat de Catalunya—AGAUR. The European Commission collaborated under projects H2020 ACTRIS-IMP (GA-871115) and H2020 ATMO-ACCESS (GA-101008004).

18 During the VORTEX-SE project, two intensive field campaigns were carried out in 2016 and 2017 [2], in which the Uni-
19 versity of Massachusetts (UMass) S-Band radar and the Collaborative Lower Atmospheric Profiling System (CLAMPS) [4]
20 yielded a wealth of observations. The key objectives encompassed the assessment of the atmospheric-boundary-layer evolution
21 and the characterization of precipitation microphysical processes in northern Alabama in the context of tornado warning and
22 monitoring [2].

23 The rainfall rate (RR) and the drop-size distribution (DSD) are key parameters that can be retrieved from vertically pointed
24 radar observations. RR estimation is influenced by the assumed DSD. In turn, the DSD can be computed from the vertically
25 pointed radar Doppler spectrum with the assumption that the drops are Rayleigh scatterers falling at their terminal velocities
26 [5]. However, in practice, the Doppler spectrum is affected by the ambient vertical air motion (VAM). Thus, given the Doppler
27 spectrum as a function of height, RR and DSD retrievals require height-dependent VAM correction. While raw velocity bins in
28 the radar observations represent a shifted, and possibly aliased, version of the mean Doppler radial velocity, velocity bins after
29 VAM correction are expected to represent the true terminal fall velocity of the raindrops.

30 Different approaches to estimate VAM have been carried out in the literature: Kim et al. [6] obtained VAM estimations
31 using Doppler spectra derived from a 1290-MHz wind profiler, which showed good agreement in comparison with the VAM
32 derived at 300 m in height from a K-band micro-rain radar and at surface from a disdrometer. They used the Sans Air Motion
33 (SAM) gamma-size hydrometeor distribution model introduced by Williams [7], who proposed a method to estimate VAM
34 based on iterative fitting the DSD retrieved from the velocity-shifted observed spectrum and the SAM-DSD model. In contrast,
35 this paper tackles VAM estimation relying on RR measurements by a ground-based disdrometer, assuming high RR correlation
36 between different measurement heights considering 5-min average ensembles. Although collision and coalescence processes
37 limit radar- and disdrometer-DSD coincidence, correlation coefficients of $\rho \simeq 0.75$ are found for the RR between disdrometer
38 and radar at 500 m in [5]. This paper is organised as follows: Sect. 2 presents the instrumentation including the OTT Parsivel2
39 disdrometer and the UMASS S-band radar, and the retrieval methods for the RR and DSD products and the VAM estimation.
40 Sect. 3 shows a case study on the proposed VAM estimation method, and Sect. 4 gives conclusion remarks.

41 2. INSTRUMENTS AND METHODS

42 2.1. The UMASS S-Band radar

43 The S-Band FMCW radar employed during VORTEX-SE was developed by the Microwave Remote Sensing Laboratory from
44 the University of Massachusetts. This radar is deployed on a truck for mobility and uses two parabolic dish antennas, both
45 with diameter of 2.4 m and gain of 34 dB, and a 250 W transmitter [3]. This system measures the volume reflectivity spectral
46 density (with respect to velocity), $\eta(v)$, with averaged spatial and temporal resolutions of 5 m and 16 s, respectively. From
47 these it is possible to obtain profiles of the spectral reflectivity factor, $Z(v)$, vertical velocity, v , and spectrum width, w . This
48 radar enables to study the atmospheric boundary layer behaviour as well as precipitation events, because it is able to detect both

49 clear-air echo and precipitation [5].

50 2.2. The OTT Parsivel2 disdrometer

51 The OTT Parsivel2 disdrometer used for VORTEX-SE measurement campaign is deployed as a part of the Portable *In situ* Pre-
52 cipitation Station (PIPS), designed and developed by Purdue University and the U.S. National Severe Storms Laboratory. This
53 is a ground-based instrument that measures optically at 1 dimension the precipitation size particle-by-particle. The disdrometer
54 has an approximate temporal resolution of $\simeq 10$ s and measures different rain-related parameters such as the DSD and the RR,
55 among others [8].

56 2.3. Data products and Vertical Air Motion correction

57 *Data products.*- The steps to estimate the RR and DSD from radar measurements begin with the measured radar volume
58 reflectivity $\eta(v)$ as a function of velocity (see details in Appendix of [5] and physical basis in [9]). The DSD is defined as

$$N(D) = \frac{\eta(D)}{\sigma(D)}, \quad (1)$$

59 where $\sigma(D)$ is the single-particle backscattering cross section of a drop of diameter D , and $\eta(D)$ is the radar reflectivity density
60 as a function of diameter. The rain rate is computed as

$$RR = \pi/6 \int_0^{\infty} N(D) D^3 v(D) dD, \quad (2)$$

61 which is essentially the third order moment of the DSD and fall velocity as a function of drop diameter, $v(D)$.

62 *VAM correction.*- The fundamental raindrop terminal-velocity-to-diameter relationship, denoted $v(D)$ in Eq. 2, assumes
63 that there is no vertical air motion [9],

$$v(D_n) = (9.65 - 10.3e^{-0.6 \cdot D_n}) \delta v(h), \quad (3)$$

64 where D_n is the raindrop diameter, $\delta v(h)$ is an air density correction for the terminal velocity as a function of height, and
65 velocities are positive down. In the presence of VAM, the Doppler velocity measured by the vertically-pointing radar is given
66 by

$$v_{Doppler} = v + v_{VAM}, \quad (4)$$

67 where $v = v(D)$ is the terminal fall velocity for raindrops of diameter D , $v_{Doppler}$ is the corresponding Doppler velocity
68 measured by the radar, and v_{VAM} is the VAM velocity. In what follows, dependency with diameter D will be skipped because
69 VAM is a property related to atmospheric dynamics and turbulence and therefore, it is equally affecting all particle sizes. Size

70 retrieval from Doppler velocity measurements must include the correction, $v = v_{Doppler} - v_{VAM}$ when computing Eq. 3
 71 inverse function, $D(v)$, and subsequent retrieval of the DSD and RR via Eq. 1 and Eq. 2, respectively. Therefore, in practice,
 72 the RR product can be defined as a function of the VAM velocity correction as $RR(VAM)$.

73 *VAM estimation.*- The VAM estimation method consists on an optimisation problem by solving Eq. 2 as a function of the
 74 VAM velocity correction. The optimization problem can be formulated as

$$VAM = \underset{VAM}{arg\ min} \ ||RR_{disdro} - RR(VAM)||^2, \quad (5)$$

75 where $RR(VAM)$ is the RR radar product obtained as a function of the VAM velocity correction solving Eq. 2. Eq. 5 above is
 76 posed assuming that RR_{disdro} and $RR(VAM)$ are correlated in height (at altitudes considerably lower than the melting layer)
 77 when considering 5-min averages. The VAM optimization is carried out by means of a constrained non-linear Least-Squares
 78 algorithm, minimizing the squared error between RR_{disdro} and $RR(VAM)$.

79 3. RESULTS AND DISCUSSION

80 The algorithm presented in subsection 2.3 has been applied to radar and disdrometer measurements (5-min averaged) taken
 81 during April 30, 2016 00:00-01:00 UTC in the context of VORTEX-SE measurement campaign. The algorithm estimated VAM
 82 values that, when used to correct the radar reflectivity measurements at 500 m height, provided RR values virtually identical
 83 to RR_{disdro} ($\|RR_{disdro} - RR(VAM)\|^2 < 0.002mm \cdot h^{-1}$). Fig. 1 compares the radar-measured RR at 500 m, with and
 84 without VAM correction (solid black and gray traces, respectively), to RR_{disdro} (dashed blue). It can be observed that without
 85 correction, radar-derived RR shows considerably lower values ($\simeq 0.1 mm \cdot h^{-1}$) compared to RR_{disdro} ($\simeq 0.4 - 0.8 mm \cdot h^{-1}$)
 86 mainly due to VAM-velocity-induced error [10]. With VAM correction, the radar-derived RR trace overlaps RR_{disdro} time
 87 series, and the estimated VAM time series is obtained (dashed brown trace), showing a nearly constant value of $\simeq 4 m \cdot s^{-1}$.
 88 The background color map depicts the 5-min averaged DSD measured by the FMCW radar after VAM correction.

89 In order to validate the VAM-corrected DSDs obtained for each 5-min average, and thus, the estimated RRs and VAM
 90 velocities, the gamma distribution parameterization of DSD was derived by means of the method of moments [11]. The gamma
 91 distribution representation of $N(D)$ is formulated as

$$N(D) = N_0 D^\mu e^{-\Lambda D}, \quad (6)$$

92 being characterized by N_0 , μ , and Λ parameters. Fig. 2 shows a DSD parameterization example in which the average DSD
 93 measured by the radar between 00:00 UTC and 00:05 UTC, with and without VAM correction (solid trace, b) and a) panels,
 94 respectively), is plotted along its gamma parameterization (dashed trace). It can be observed that without VAM correction
 95 (Fig. 2 a)) the measured DSD is poorly fitted to a gamma distribution, showing a great bias between the modelled and measured

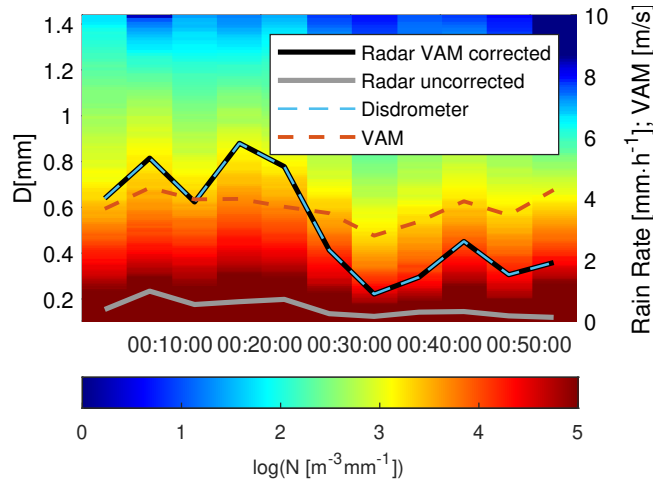


Fig. 1. Time series representing the radar-measured RR, with and without VAM correction, the disdrometer-measured RR and the VAM estimation results. The DSD is represented on the background.

96 DSDs. This is further evidenced by the gamma distribution parameters obtained, with $\mu = -3.574$ which is out of the accepted
 97 range in the literature for μ values ($\mu \in [-3, 8]$) [9]. On the other hand, after VAM correction (Fig. 2 b)), the obtained DSD can
 98 be nicely fitted to a gamma distribution. This result is quantitatively validated as well by the gamma distribution parameters
 99 obtained, now with $\mu = -2.185$ within the expected ranges.

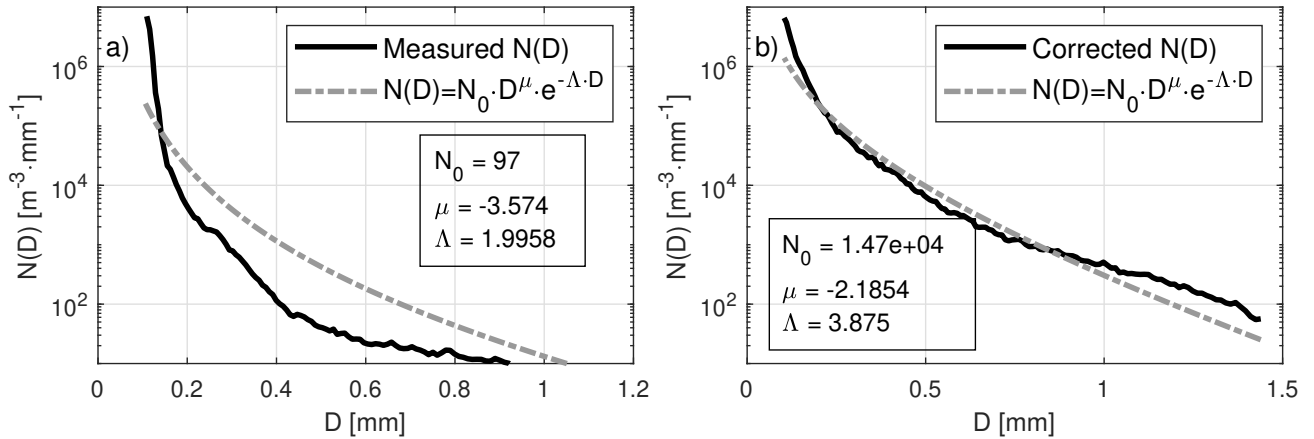


Fig. 2. Case example showing the gamma distribution fitting to a radar-measured DSD without (panel a)) and with (panel b)) VAM correction.

100 Table 1 depicts the gamma distribution parameters obtained for each of the 5-min averaged DSD measurements after VAM
 101 correction. N_0 values range from a minimum of $5.94 \cdot 10^3$ at 00:35 UTC, corresponding to the lowest RR within the measurement
 102 period under study, to a maximum of $6.66 \cdot 10^4$. μ values remain approximately constant around $\mu = -2$, and finally, Λ ranges
 103 from a minimum of 3.87 at 00:05 UTC to a maximum of 7.44 at 00:55 UTC. The obtained values are in accordance with the
 104 ranges found in the literature [9] and their temporal correlation seem to validate the VAM estimations obtained. However, all we
 105 have shown is that the radar-derived RR can be made to match the disdrometer-derived RR, and that the resulting radar-derived

Time (UTC+2)	N_0	μ	Λ
00:05:00	$1.47 \cdot 10^4$	-2.19	3.87
00:10:00	$3.15 \cdot 10^4$	-2.19	4.50
00:15:00	$2.33 \cdot 10^4$	-2.12	4.49
00:20:00	$5.76 \cdot 10^4$	-1.91	5.07
00:25:00	$3.95 \cdot 10^4$	-1.97	4.78
00:30:00	$1.43 \cdot 10^4$	-2.19	4.58
00:35:00	$5.94 \cdot 10^3$	-1.99	4.58
00:40:00	$8.85 \cdot 10^3$	-2.01	4.5
00:45:00	$1.45 \cdot 10^4$	-2.33	4.53
00:50:00	$2.35 \cdot 10^4$	-1.53	5.45
00:55:00	$6.66 \cdot 10^4$	-1.99	7.44

Table 1. Gamma distribution N_0 , μ , and Λ fit parameters found for the VAM-corrected radar-measured DSDs for the measurement period under study (April 30, 2016 00:00-01:00 UTC) in the context of VORTEX-SE campaign. Each row corresponds to a DSD 5-minute average.

106 DSD seems realistic. The Gamma distribution parameters obtained still need to be validated according to the rain type present
107 in the scenario under study, and the DSDs from the two instruments should be compared in light of their respective sensitivities.
108 The rather substantial apparent VAM over the course of 1 hour also deserves further investigation.

109 4. CONCLUSIONS

110 A methodology to estimate VAM velocity from radar and disdrometer RR measurements has been presented. The method
111 consists on fitting the radar-retrieved RR, as a function of VAM velocity correction, to the disdrometer-measured RR using
112 constrained non-linear Least-Squares optimization.

113 The methodology was tested over experimental data captured during a 1-hour period by an S-band FMCW radar and an OTT
114 Parsivel2 disdrometer in the context of VORTEX-SE measurement campaign. The estimation results found a nearly constant
115 VAM velocity of $\simeq 4$ m/s during the observation period. After VAM correction, the radar-measured RR was found to match
116 almost ideally the disdrometer-measured RR. In order to validate these results, the gamma distribution parameterization was
117 derived for each of the estimated DSD. It was found that without VAM correction, the gamma distribution parameters showed
118 unrealistic values, outside of the accepted bounds for a precipitation process. On the other hand, after VAM-correction, realistic
119 values for all parameters were found with a coherent temporal continuity, showing the methodology improvement of the radar
120 measurements.

121 Although good performance of the algorithm has been observed, it needs to be tested over different experimental data,
122 validating the VAM estimations by means of radar wind profilers. Moreover, the effect of reflectivity density aliasing needs to
123 be studied as well.

5. REFERENCES

- 125 [1] U. Löhnert and O. Maier, “Operational profiling of temperature using ground-based microwave radiometry at Payerne:
126 Prospects and challenges,” *Atmos. Meas. Tech.*, vol. 5, pp. 1121–1134, May 2012.
- 127 [2] R. L. Tanamachi, S. J. Frasier, J. Waldinger, A. LaFleur, D. D. Turner, and F. Rocadenbosch, “Progress toward Character-
128 ization of the Atmospheric Boundary Layer over Northern Alabama Using Observations by a Vertically Pointing, S-Band
129 Profiling Radar during VORTEX-Southeast,” *J. Atmos. Ocean. Technol.*, vol. 36, no. 11, pp. 2221–2246, 2019.
- 130 [3] T. İnce, S. J. Frasier, A. Muschinski, and A. L. Pazmany, “An S-band frequency-modulated continuous-wave boundary
131 layer profiler: Description and initial results,” *Radio Sci.*, vol. 38, no. 4, 2003.
- 132 [4] T. J. Wagner, P. M. Klein, and D. D. Turner, “A new generation of ground-based mobile platforms for active and passive
133 profiling of the boundary layer,” *Bull. Am. Meteorol. Soc.*, vol. 100, no. 1, pp. 137–153, 2019.
- 134 [5] F. Rocadenbosch, R. Barragán, S. J. Frasier, J. Waldinger, D. D. Turner, R. L. Tanamachi, and D. T. Dawson, “Ceilometer-
135 based rain-rate estimation: A case-study comparison with s-band radar and disdrometer retrievals in the context of vortex-
136 se,” *IEEE Trans. Geosci. Remote Sens.*, vol. 58, no. 12, pp. 8268–8284, 2020.
- 137 [6] D.-K. Kim and D.-I. Lee, “Raindrop size distribution properties associated with vertical air motion in the stratiform
138 region of a springtime rain event from 1290 mhz wind profiler, micro rain radar and parsivel disdrometer measurements,”
139 *Meteorol. Appl.*, vol. 23, no. 1, pp. 40–49, 2016.
- 140 [7] C. R. Williams, “Simultaneous ambient air motion and raindrop size distributions retrieved from uhf vertical incident
141 profiler observations,” *Radio Sci.*, vol. 37, no. 2, pp. 1–22, 2002.
- 142 [8] A. Tokay, D. B. Wolff, and W. A. Petersen, “Evaluation of the new version of the laser-optical disdrometer, ott parsivel2,”
143 *Journal of Atmospheric and Oceanic Technology*, vol. 31, no. 6, pp. 1276 – 1288, 2014.
- 144 [9] R. J. Doviak *et al.*, *Doppler radar and weather observations*. Courier Corporation, 2006.
- 145 [10] D. Rajopadhyaya, P. May, R. Cifelli, S. Avery, C. Willams, W. Ecklund, and K. Gage, “The effect of vertical air mo-
146 tions on rain rates and median volume diameter determined from combined uhf and vhf wind profiler measurements and
147 comparisons with rain gauge measurements,” *J. Atmos. Ocean Technol.*, vol. 15, 12 1998.
- 148 [11] A. Tokay and D. A. Short, “Evidence from tropical raindrop spectra of the origin of rain from stratiform versus convective
149 clouds,” *Journal of Applied Meteorology and Climatology*, vol. 35, no. 3, pp. 355 – 371, 1996.